

A Comparison of Tsunami Impact to Sydney Harbour, Australia at Different Tidal Stages

Olivia A. Wilson, Hannah E. Power, Murray Kendall

Abstract—Sydney Harbour is an iconic location with a dense population and low-lying development. On the east coast of Australia, facing the Pacific Ocean, it is exposed to several tsunamigenic trenches. This paper presents a component of the most detailed assessment of the potential for earthquake-generated tsunami impact on Sydney Harbour to date. Models in this study use dynamic tides to account for tide-tsunami interaction. Sydney Harbour's tidal range is 1.5 m, and the spring tides from January 2015 that are used in the modelling for this study are close to the full tidal range. The tsunami wave trains modelled include hypothetical tsunami generated from earthquakes of magnitude 7.5, 8.0, 8.5, and 9.0 M_w from the Puységur and New Hebrides trenches as well as representations of the historical 1960 Chilean and 2011 Tohoku events. All wave trains are modelled for the peak wave to coincide with both a low tide and a high tide. A single wave train, representing a 9.0 M_w earthquake at the Puységur trench, is modelled for peak waves to coincide with every hour across a 12-hour tidal phase. Using the hydrodynamic model ANUGA, results are compared according to the impact parameters of inundation area, depth variation and current speeds. Results show that both maximum inundation area and depth variation are tide dependent. Maximum inundation area increases when coincident with a higher tide, however, hazardous inundation is only observed for the larger waves modelled: NH90high and P90high. The maximum and minimum depths are deeper on higher tides and shallower on lower tides. The difference between maximum and minimum depths varies across different tidal phases although the differences are slight. Maximum current speeds are shown to be a significant hazard for Sydney Harbour; however, they do not show consistent patterns according to tide-tsunami phasing. The maximum current speed hazard is shown to be greater in specific locations such as Spit Bridge, a narrow channel with extensive marine infrastructure. The results presented for Sydney Harbour are novel, and the conclusions are consistent with previous modelling efforts in the greater area. It is shown that tide must be a consideration for both tsunami modelling and emergency management planning. Modelling with peak tsunami waves coinciding with a high tide would be a conservative approach; however, it must be considered that maximum current speeds may be higher on other tides.

Keywords—Emergency management, Sydney, tide-tsunami interaction, tsunami impact.

I. INTRODUCTION

THE city of Sydney in New South Wales (NSW) is Australia's most populated city and home to the picturesque Sydney Harbour (Port Jackson) (Fig. 1). Sydney Harbour is both a working port and major location for

recreational boating and leisure with large numbers of people on and around the water every day.

There is geological and historical evidence for tsunami affecting the NSW coastline, and the NSW State Emergency Services (SES) Tsunami Emergency Sub Plan estimates that a large tsunami with the potential to impact the entire NSW coast would directly threaten between 250,000 and 1.5 million people [1]. Although the threat is considered moderate, it is real. One of the most catalogued historic tsunami events to affect Sydney Harbour is the Chilean tsunami of May 1960 [2]. The 1960 Chilean tsunami was caused by a subduction zone earthquake, as are the majority (~73%) of tsunami globally [3]. Tsunamis are also known to be caused by submarine landslides, undersea volcanoes, asteroid impacts, and other sources [4], [3]. Accounts from the 1960 Chilean event are detailed in [2] and include reports of unusual wave heights, extreme currents, and rapid changes in water level. The effects of this tsunami include dragged and broken moorings, vessels being swept into bridges and wharfs, as well as significant scouring and localised coastal erosion.

T2 is a second generation database of tsunami scenarios developed by the Joint Australian Tsunami Warning Centre (JATWC) to aid the national tsunami warning service for Australia. Tsunami scenarios are modelled from earthquakes of 7.5, 8.0, 8.5, and 9.0 M_w from relevant source zones and can be extracted at any deep water location requested [5]. Shallow water inundation modelling is required to determine the impacts of these tsunami scenarios.

There are several programs available to accurately model potential tsunami. The open source software ANUGA is a widely used hydrodynamic model that has been validated for tsunami propagation and inundation [6], [7]. For tsunami propagation and transformation, ANUGA solves the non-linear shallow water wave equations, which have been shown to provide a good description of tsunami behaviour [9].

It is common to model tsunami wave trains with a static tide, e.g. [9], [10]. Tide and tsunami wave trains have significant differences in wavelength, and so, it can be assumed that the interaction is negligible or it may be difficult to incorporate into a model and so is acknowledged as a limitation. It has, however, been shown that tsunami wave trains and tide interact in a non-linear manner in estuaries. Coupling tide and tsunami for estuary models, such as this study for Sydney Harbour, can therefore reduce the limitations of the model [11]-[13].

Preliminary modelling in Sydney Harbour showed that inundation extents differed according to which tidal stage the peak tsunami waves coincided with, warranting further

O. A. Wilson, PhD candidate, H. E. Power, lecturer, M. Kendall, honour's student, are with the University of Newcastle, Callaghan, NSW 2308, Australia (e-mail: olivia.wilson@newcastle.edu.au, hannah.power@newcastle.edu.au, murray.kendall@uon.edu.au).

investigation. It is important to know the ways in which tidal stage influences the potential impact of a tsunami from both an emergency management and research perspective. Shallow water tsunami modelling is computationally intensive and

requires large amounts of processing time. Knowledge of tidal influence on tsunami impact can aid the researcher to select optimum input variables for efficient modelling and inform the interpretation of results.

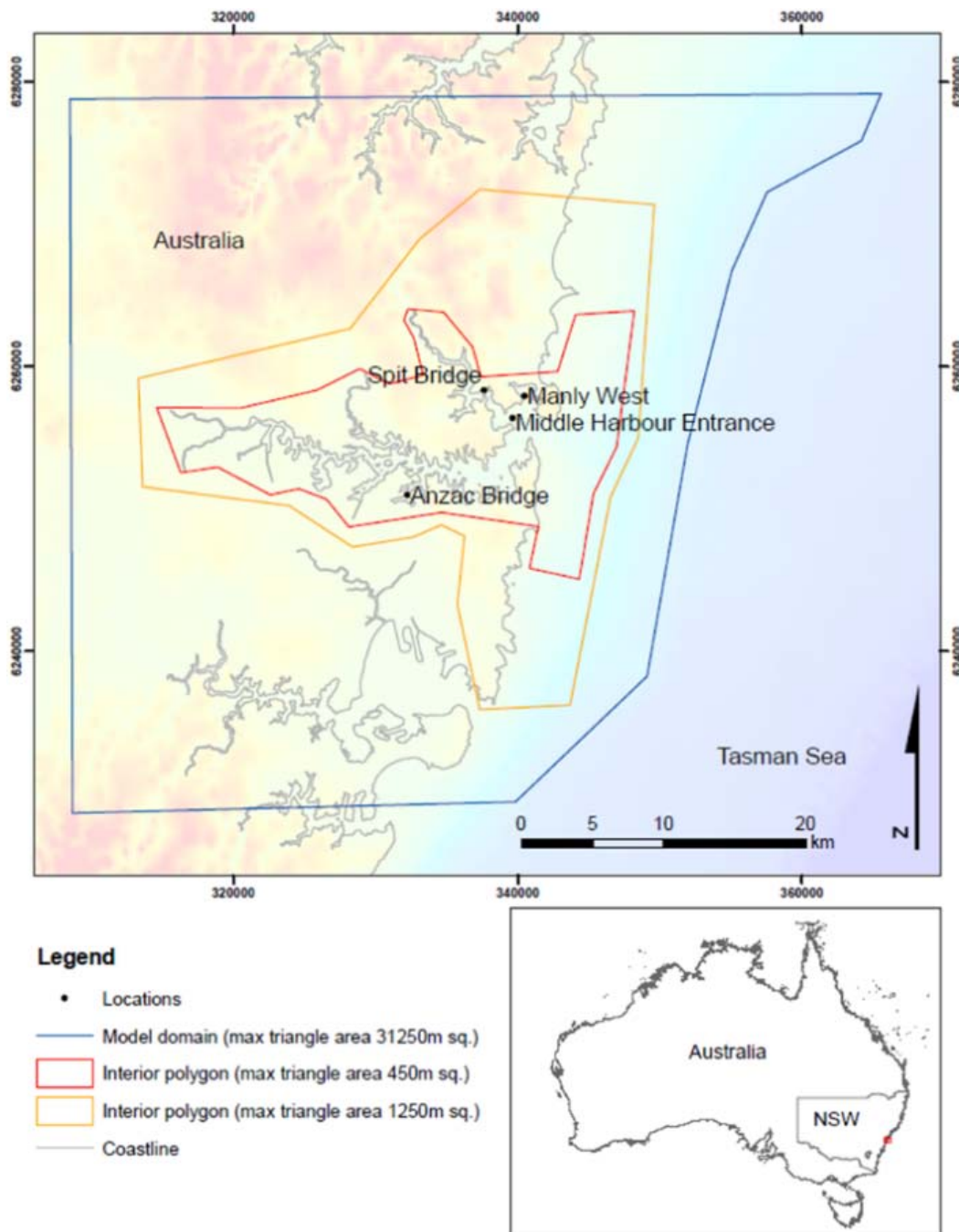


Fig. 1 Study site and locations selected to represent potential tsunami impact within the context of the model domain

This paper focusses on the sensitivity of maximum inundation area, depth variation and maximum current speeds to tide-tsunami phasing in the context of a Sydney Harbour tsunami modelling project.

II. METHODS

Tsunami inundation models were setup using the open source hydrodynamic model, ANUGA. ANUGA is a widely used hydrodynamic model that has been validated for tsunami

propagation and inundation [6], [7]. For tsunami propagation and transformation, ANUGA solves the non-linear shallow water wave equations, which have been shown to provide a good description of tsunami behaviour [8].

The ANUGA model requires the following inputs: bathymetry/topography, tsunami wave train boundary conditions, tidal water level, and area delimited friction values.

A. Bathymetry and Topography Data

Bathymetry and topography data were sourced and then collated using ESRI ArcGIS 10.1™. Data were adjusted or reprojected so that all data conformed to the vertical datum Australian Height Datum (AHD) and the horizontal projection WGS84 UTM zone 56. Topographic and bathymetric data resolutions range from 1m to 250 m. The datasets used to form the compilation were the most recent and highest quality available to this project. Grid compilation resolutions were selected as the highest resolution possible whilst maintaining the accuracy of the underlying data. For the input topographic data, this resolution was <10 m and for the bathymetry <30 m. The triangular mesh generated by ANUGA had triangles with a maximum area of 450 m². The model domain is illustrated in Fig. 1.

B. Tsunami Wave Train Boundary Conditions

The T2 tsunami wave database was used to provide tsunami wave trains for the ANUGA inundation model. T2 follows T1 as a second generation tsunami scenario database developed as a part of the Joint Australian Tsunami Warning Centre (JATWC). T2 was developed to provide numerical guidance for Australia's tsunami warning service. The database holds a total of 1,865 individual scenarios from 522 source locations for earthquakes of magnitude 7.5, 8.0, 8.5, and 9.0 M_w. These include historical scenarios which may be adjusted to fit historical data records.

Rupture modelling is based on the relationship between magnitude and rupture dimensions as described in [5]. The MOST model is then used to predict tsunami propagation from source to location and a tsunami wave time series is extracted at a location along the 100-m depth contour offshore Sydney Harbour. This time series is then used as a boundary condition (at the 100m depth contour) for the ANUGA tsunami inundation models presented in this study.

Wave trains were selected for the two source zones known to be the greatest threat to Sydney Harbour: Puysegur and New Hebrides [14]. Two historical events were also selected: the 2011 Tohoku Japanese event and the 1960 Chilean event.

C. Tide Data

A variable tidal water level was incorporated into the models to account for the interaction between the tide and the tsunami wave train.

Models for all wave trains (7.5 M_w, 8.0 M_w, 8.5 M_w, and 9.0 M_w earthquake generated tsunami from the Puysegur and New Hebrides trenches) were run so that the cluster of large waves coincided with both a tidal trough (low tide) and a tidal peak (high tide). This sequence of results is referred to as the

high/low series. To complement this series, a model was run with tide data only.

The wave train representing a tsunami from a 9.0-M_w earthquake at the Puysegur trench was modelled for the peak waves to coincide with the tidal phase that occurs at every hour across a 12-hour tidal wavelength. This series of results is referred to as the P90h± series.

The tide data used were one wavelength (~12 hours) of the largest wave (by height from trough to peak) extracted from the spring tides of January 2015 for the Sydney Harbour tide gauge (151°15'30.72", -33°49'31.56"). Tide data were adjusted from the local datum (Zero Fort Denison) to MSL, a difference of 0.925 m and then summed to the T2 wave train. A model was run with only tide data entered at the 100-m depth contour boundary and no tsunami wave train as a point of comparison for the model outputs. Wave data were then extracted at the position of the relevant tide gauges and found to range from 0-7 cm variation from the tidal input, with a mean of 1 cm variation. This was considered suitable verification of the tidal input data.

D. Friction

A Manning's *n* value of 0.02 was used across the entire model domain. This value was shown through investigation by [9] to be suitable for seabed roughness, road surfaces, and sand/gravel.

E. Model Outputs

The ANUGA model output file is in NetCDF format and pertains to a set of positions and a set of times at which the model is evaluated. The output file can then be interrogated to extract the results required.

Results were extracted for the model domains for specific locations to provide data on inundation extents, current speeds and depth variation. These data were then interpreted to create inundation maps and data time series as required.

III. RESULTS

ANUGA solves the non-linear shallow water wave equations to describe the tsunami behaviour for each node in the elevation mesh and each time step over a specified period. These calculations were completed for every scenario modelled, and results were extracted to describe inundation, current speeds, and depth variation across the study site.

Wave trains modelled are described in Tables I and II:

A. Maximum Inundation

Maximum inundation extent maps of all scenarios modelled were generated and examined. Maximum area inundated was calculated above the high tide line for all inundation extent maps to provide a site-specific relative measure.

It is clear that maximum inundation extents are dependent on tidal phase. For the wave trains modelled to coincide with high tide, significantly more inundation occurred. The majority of wave trains modelled on a low tide only show isolated inundation, with hazardous inundation only occurring

for scenarios with the largest wave heights (NH90low and P90low) (Fig. 2).

The P90h± series shows a clear trend for maximum inundation area. Fig. 3 illustrates inundation area peaking at high tide and decreasing as the peak tsunami wave moves closer to the low tide.

TABLE I
WAVE TRAINS MODELLED (HIGH/LOW SERIES)

Scenario Name	Source Zone	T2 Source M _w	PTHA ~ARI	Input wave parameters (m)	
				H _{rms} (m)	H _{max} (m)
Scenarios					
P75high P75low	Puysegur	7.5	25	0.01	0.05
P80high P80low	Puysegur	8.0	50	0.05	0.18
P85high P85low	Puysegur	8.5	200	0.17	0.53
P90high P90low	Puysegur	9.0	4700	0.44	1.36
NH80high	New	8.0	30	0.04	0.14
NH80low	Hebrides				
NH85high	New	8.5	110	0.16	0.48
NH85low	Hebrides				
NH90high	New	9.0	550	0.37	1.00
NH90low	Hebrides				
Historical Events					
Chi1960high	Chile		70	0.10	0.40
Chi1960low					
Toh2011high	Japan		35	0.05	0.14
Toh2011low					

Details wave trains modelled in the high/low series. Wave train names are given for 'high' and 'low' scenarios, where 'high' represents the peak tsunami waves train coinciding with high tide and 'low' represents coincidence with low tide. PTHA ~ ARI represents the Annual Recurrence Interval as estimated by the Probabilistic Tsunami Hazard Analysis of Australia [14].

TABLE II
9.0-M_w PUYSEGUR WAVE TRAIN AND TIDAL PHASES MODELLED (P90h± SERIES)

Wave Train Name	Tidal Phase (offset hours relative to high tide)
P90no	No tide
P90h-4	-4
P90h-3	-3
P90h-2	-2
P90h-1	-1
P90high	0
P90h+1	1
P90h+2	2
P90h+3	3
P90h+4	4
P90h+5	5
P90low	6
P90h+7	7

B. Maximum and Minimum Depths

Maximum and minimum depths were calculated for a series of locations in the model domain (Fig. 1). The Spit Bridge, which has high vessel traffic passing underneath it, has a clearance of ~7 m at MSL [15] and was selected as a suitable location to illustrate the hazard of depth variation. There are also several marinas and numerous vessel moorings in the Spit Bridge area.

Fig. 4 is a time series that illustrates both the depth variation and the rapidity of depth changes for the high/low series. For clarity, only the Puysegur wave series is shown.

For the high/low series, tsunami occurring at high tide show hazardous maximum depths and tsunami occurring at low tide, hazardous minimum depths. For example, the scenario P90high shows depths between 5.3 and 9.3 m, where 9.3 m is over 2 m higher than the high tide water level. P90low shows depths between 3.4 and 7.2 m. A minimum depth of 3.4 m is over 1.7 m shallower than the low tide water level. For this location, the depth ranges are only significantly different to depths experienced under non-tsunamagenic conditions for scenarios sourced from earthquakes of 8.5 M_w and greater. Other scenarios show depth ranges outside the normal tidal oscillation of the order of centimetres.

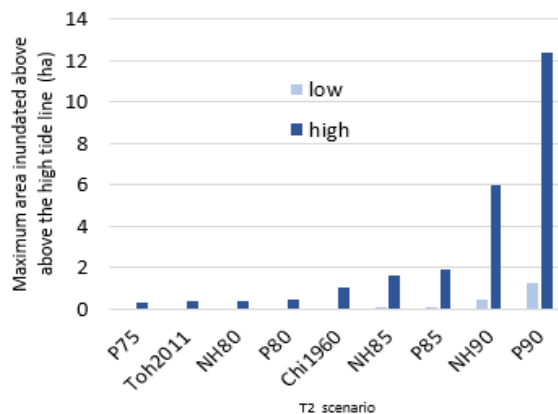


Fig. 2 Maximum area inundated above the high tide line, for the high/low series. The high tide line was extracted from a model running only tide and no tsunami scenario

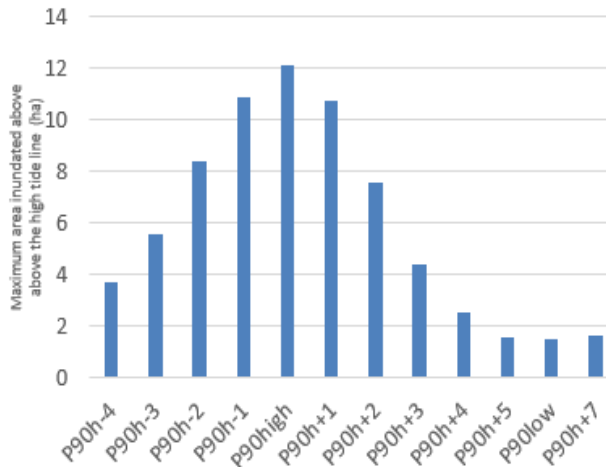


Fig. 3 Maximum area inundated above the high tide line for the P90h± series

The P90h± series in Fig. 5 shows a clear pattern determined by the tide. Tsunami that coincide with higher tidal water levels have depth ranges with greater maximum and minimum depths. For tsunami that coincides with lower tidal water levels, the range of depths is shallower. The difference between maximum and minimum depths varies (3.5-4.6 m) although not significantly.

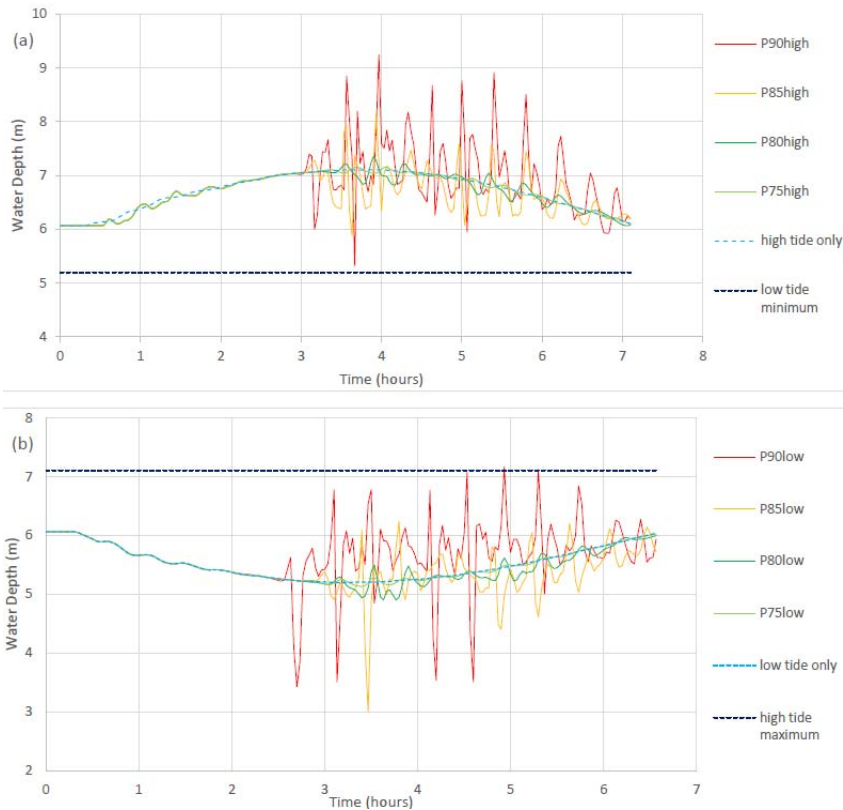


Fig. 4 Depth variation for Puysegur waves from the high/low series at the Spit Bridge location for a) tsunami scenarios coincident with a high tide and b) tsunami scenarios coincident with a low tide

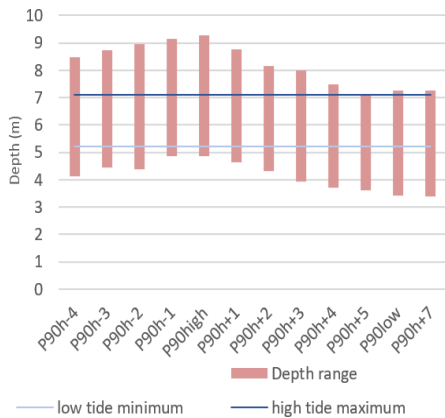


Fig. 5 Maximum and minimum water depths for the P90h± series at the Spit Bridge location

For the P90h± series, maximum water depth exceeds 2 m higher than high tide levels for scenarios P90h-1 and P90high. Minimum water depths are more than 1.5 m shallower than low tide for scenarios P90h+4, P90h+5, P90low, and P90h+7.

C. Maximum Current Speeds

Maximum current speeds were extracted for specific locations that are centres of marine infrastructure and/or areas that experience high current speeds in preliminary modelling.

Results from the two locations, Spit Bridge and Middle Harbour Entrance, are shown as examples.

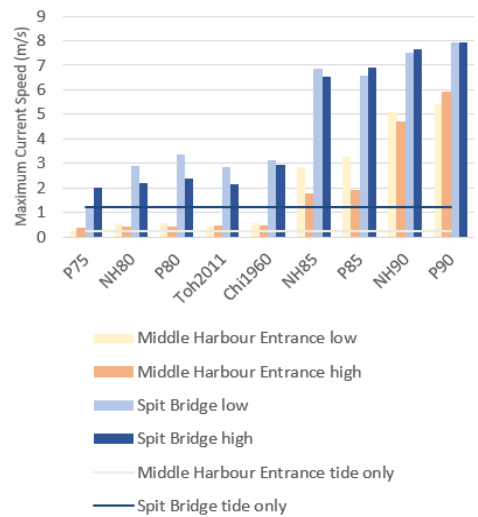


Fig. 6 Maximum current speeds for the high/low series at locations Spit Bridge and Middle Harbour Entrance

For the high/low series, there is no consistent pattern between scenarios modelled across a high or low tide (Fig. 6). At the Spit Bridge, scenarios NH80, P80 Toh2011 and Chi1960 all show higher maximum current speeds when

coincident with a low tide, but the difference is not significant. The tsunami scenarios with larger waves (NH85, P85, NH90 and P90) also show minimal difference between coincidence with a high or low tide.

At Middle Harbour Entrance, maximum current speeds are <1 m/s for waves P75, NH80, P80, Toh2011, and Chi1960 and differences between scenarios coincident with high and low tides are both small and inconsistent. For scenarios NH85 and P85, maximum current speeds are higher when coincident with a low tide rather than a high tide. Scenario NH90 shows higher current speeds when modelled across a low tide, and scenario P90 shows higher current speeds when modelled across a low tide.

The P90h± series for these two locations does not show a pattern that is clearly determined by incremental changes in tide (Fig. 7). At the Spit Bridge, maximum current speeds range between 8.0 and 8.3 m/s, with only 0.3 m/s between the highest and lowest current speeds. Middle Harbour Entrance shows a greater range of values (5.3-6.7 m/s) but also did not show a clear pattern with respect to tsunami-tidal phasing.

IV. DISCUSSION

This paper presents results from the most detailed assessment to date of the potential earthquake-generated tsunami impact on Sydney Harbour. Using site specific modelling to compare potential impact at different tidal stages provides both scientists and emergency managers with an evidence base on which to inform research and planning. The results of this paper can therefore be used to prioritise future modelling efforts.

Results show that the extent of the tsunami threat to Sydney Harbour is tide dependent. The tidal phase coincident with the largest waves in a tsunami wave train will determine both the extent of land inundation and maximum and minimum water depths. Inundation results are consistent with the trends in inundation results showed by previous modelling using a static tide for the Manly area (a subsection of the model domain for this study) and Botany Bay [9], [10] as well as previous modelling across the same model domain with waves sourced from the TsuDAT database [16]. Further research is required to determine the differences in inundation results for models using a static or dynamic tide for Sydney Harbour.

Maximum current speeds do not show tide dependence but are more likely to be influenced by other variables such as morphology and water depth. Consistent with previous studies, larger tsunami input waves produce higher maximum current speeds [16], [9], [17]. These impacts have the potential to create hazards for shipping and other water users. The combination of current speeds and rapid changes in water level considered responsible for the damage caused by the historic 1960 Chilean tsunami during which vessels were torn from moorings, swept under bridges and collided with infrastructure [2].

For conservative modelling, our results suggest that tsunami should be modelled to coincide with high tides; however, it should be acknowledged that maximum current speeds may be higher for tsunami waves coincident with other tidal phases. If

maximum current speeds are of particular interest, models should coincide tsunami waves with a spread of different tidal phases and consider other factors influencing current speeds, such as those determined by location.

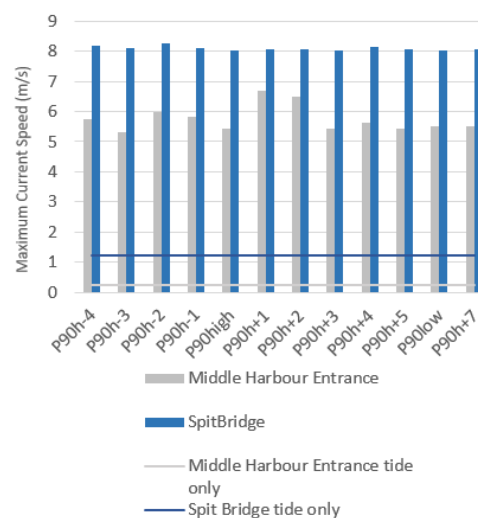


Fig. 7 Maximum current speeds for the P90h± series at Spit Bridge and Middle Harbour Entrance locations

The results should be viewed with respect to model limitations that include accuracy of the input elevation data, which was the best available, but may have errors. Mesh resolution was $\sim 30 \text{ m}^2$ due to limitations with computing resources. The tsunami scenarios modelled only include those sourced from the T2 database, which are generated using the same technique. These scenarios also only represent tsunami generated by earthquakes and do not include other sources such as submarine landslides, volcanoes, or asteroid sources.

ACKNOWLEDGMENT

This research partially funded by the NSW Government under the State Emergency Management Projects program. We have also gratefully received support and data from NSW Office of Environment and Heritage (OEH), Geoscience Australia (GA), NSW State Emergency Services (SES) and the Bureau of Meteorology (BOM). The individuals from those organisations who have helped enormously include David Hanslow and Edwina Foulsham from OEH and Jane Sexton and Gareth Davies from GA, Nick Kuster and David Bowing from the SES and Diana Greenslade and Stewart Allen from the BOM. Aaron Scott and the Academic and Research Computing Services team at the University of Newcastle has also been instrumental with the IT and model setup. Thanks also goes to organisations other than those above that have contributed data: Sydney Water, Roads and Maritime Services, Manly Hydraulics Laboratory and the Port Authority of NSW.

REFERENCES

- [1] NSW SES State Emergency Management Committee. "New South Wales Tsunami Emergency SubPlan," A Subplan of the New South Wales Disaster Plan (DISPLAN), 2008.
- [2] B. Beccari, "Measurements and Impacts of the Chilean Tsunami of May 1960 in New South Wales, Australia." Report by NSW SES, State Headquarters, 2009.
- [3] UNESCO. "International Tsunami Information Centre," Available at http://itic.ioc-unesco.org/index.php?option=com_content&view=category&layout=blog&id=1160&Itemid=1077&lang=en, (Accessed: December, 2015).
- [4] D. Dominey-Howes, "Geological and historical records of tsunamis in Australia," *Marine Geology*, vol. 239(1-2), pp. 99-123, 2007.
- [5] D. Greenslade, M. Simanjuntak and S. Allen, "An Enhanced Tsunami Scenario Database: T2," CAWCR Technical Report No. 014, 2009.
- [6] B. Hinwood and E. Maclean. "Effects of the March 2011 Japanese Tsunami in Bays and Estuaries of SE Australia," *Pure and Applied Geophysics*, vol. 170, 6-8, pp. 1207-1227, 2012.
- [7] O. Nielsen, S. Roberts, D. Gray, A. McPherson and A. Hitchman. MODSIM 2005 International Congress on Modelling and Simulation Modelling Society of Australia and New Zealand, pp. 519-523, 2005.
- [8] V. V. Titov and C. E. Synalakis, "Numerical modelling of tidal wave runoff," *Journal of Waterway, Port, Coastal and Ocean Engineering*, vol. 124(4), pp. 157-171, 1988.
- [9] Cardno. "NSW Tsunami Inundation Modelling and Risk Assessment". NSW State Emergency Service and Office of Environment and Heritage Report, 2008.
- [10] F. Dall'Osso, D. Dominey-Howes, C. Moore, S. Summerhayes and G. Withycombe. "The exposure of Sydney (Australia) to earthquake-generated tsunamis, storms and sea-level rise: a probabilistic multi-hazard approach." *Sci Rep*, vol. 4, pp. 7401, 2014.
- [11] Z. Kowalik and A. Proshutinsky. "A. Tsunami-tide interactions: A Cook Inlet case study" *Continental Shelf Research* vol. 30(6), pp 633-642, 2010.
- [12] P. Myers and A. Baptista "Analysis of Factors Influencing Simulations of the 1993 Hokkaido Nansei-Oki and 1964 Alaska Tsunamis," *Natural Hazards*, vol. 23, pp 1-28, 2001.
- [13] Y. J. Zhang, R. C. Witter, G. R. Priest, "Tsunami-tide interaction in 1964 Prince William Sound tsunami," *Ocean Modelling*, vol. 40, pp. 246-259, 2011.
- [14] D. Burbidge, R. Mieczko, C. Thomas, P. Cummins, O. Nielsen and T. Dhu, "A Probabilistic Tsunami Hazard Assessment for Australia." Geoscience Australia Report, 2008.
- [15] NSW Maritime. Bridge Opening Times, Available at <http://www.rms.nsw.gov.au/maritime/using-waterways/bridge-opening-times.html>, Accessed: February, 2016.
- [16] H. Power, O. Wilson, K. Mollison, "Tsunami inundation in estuaries and coastal rivers: improved guidelines and attenuation rules," School of Environmental and Life Sciences, University of Newcastle, State Emergency Management Project Report, 2016.
- [17] O. Wilson, H. Power. "Tsunami Inundation Modelling in Estuaries: Sensitivity to Variations in Tide from an Emergency Management Perspective," *Journal of Coastal Research*, vol. 75, pp. 1262-1266, 2016.